

Vision-based Automatic Forming of Rheological Objects Using Deformation Transition Graphs

Shinichi Tokumoto, Takuya Saito, and Shinichi Hirai

Dept. of Robotics,
Ritsumeikan Univ., Kusatsu, Shiga 525-8577, Japan
E-mail: gr082982@se.ritsumei.ac.jp

Abstract

Manipulative operations of rheological objects can be found in many industrial fields such as food industry and medical product industry. Automatic operations of rheological objects are eagerly required in these fields. In this paper, we will realize a vision-based automatic forming of rheological objects using deformation transition graphs.

First, we will develop forming machine of rheological objects with multi degrees of freedom. Secondly, we will analyze the forming processes of rheological objects. Thirdly, we will introduce a deformation transition graph so that the forming processes can be described in a systematic manner. Finally, we will propose a forming control method of a rheological object based on the deformation transition graph.

1 Introduction

In food industry, we can find many manipulative operations that deal with deformable rheological materials such as dough, paste, jelly, and meat. Most these operations are done by humans. Especially, operations with large deformation of rheologic objects depend upon humans. For example, forming of pizza dough to a thin circular shape is performed by humans while extension of the dough can be done by mechanical stretchers. Thus, automatic operations by machines are strongly required for the purpose of cost reduction and cleanness of food.

Object deformation has been investigated in various research fields. Modeling of viscoelastic objects has been studied in computer graphics [1, 2] and virtual reality [3]. These researches focus on the deformation modeling of viscoelastic objects and forming operations of viscoelastic objects are out of consideration. Thus, we have no method to determine a forming strategy based on the object model. Material nature of rheologic objects is investigated extensively in rheology [4]. Unfortunately, deformation of rheologic objects in 3D space is not studied in rheology. Handling operations of deformable objects have been studied recently. Automatic handling of deformable parts in garment industry and shoe industry has been experimentally studied [5, 6]. Zheng and Chen have proposed a strategy to insert a deformable beam into a hole [7]. Wada et al. have proposed a control law

for the positioning operation of extensible clothes [8]. These researches focus on handling of elastic objects and forming operations of rheologic objects are out of focus.

In this paper, we will focus on the automatic forming operation of rheologic objects. First, we will develop forming machine of rheological objects with multi degrees of freedom. Secondly, we will analyze the forming processes of rheological objects. Thirdly, we will introduce a deformation transition graph so that the forming processes can be described in a systematic manner. Finally, we will propose a forming control method of a rheological object based on the deformation transition graph.

2 Development of Forming Machine with Multi Degrees-of-Freedom

In this section, we will develop forming machine of rheological objects with multi degrees of freedom.

Figure 1 shows the configuration between a cylindrical roller and a planar table. The roller has six degrees of freedom relative to the table; three for translation and three for rotation. Traditional stretchers have two degrees of freedom; The five freedoms can be assigned to either a roller or a table. Note that feed motion T_1 is assigned to a table in stretchers. Translational freedom T_1 is thus assigned to a table. Rotation around a vertical axis is involved in planar motion in the table plane. Rotational freedom R_2 is thus assigned to the table. The other freedoms T_2 and R_1, R_3 are not planar motion in the table plane. Freedoms T_2 and R_1, R_3 are thus assigned to a roller. Consequently, a table should have three degrees of motion, T_1 and R_2 , while a roller should have the other degrees of freedom, T_2 and R_1, R_3 .

Based on the above investigation, we will develop a forming machine illustrated in Figure 2, where the five freedoms can be controlled to change the configuration between a roller and a table. A roller is supported by a link mechanism with rotational joints a_1, a_2 , and a_3 and prismatic joints b_1 and b_2 . All rotational joints are passive while two prismatic joints are driven by actuators. The distance between the roller and the table as well as the angle from the horizon of the roller can be changed by controlling the two actuators, which drive

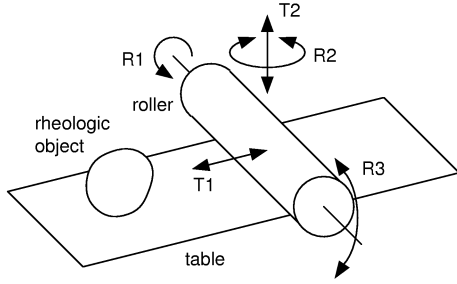


Figure 1: Motion freedoms of forming machine

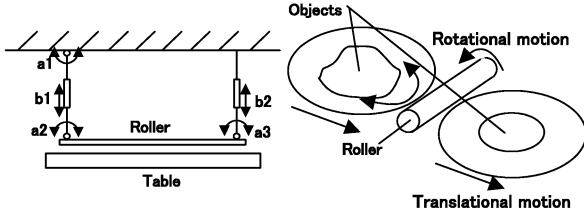


Figure 2: Mechanism of proposed forming machine

prismatic joints b_1 and b_2 . As a result, translation T_2 and rotation R_2 are controllable in the proposed mechanism. A circular table can rotate around its axis and can translate reciprocally along the table plane. Namely, rotation R_2 and translation T_1 are controllable in the mechanism. These four effective freedoms are driven by DC servo motors, which are controlled from a PC through a D/A converter. Rotation R_1 and translation T_1 are synchronized by a driving belt. Thus, the tangential speed at the surface of the roller coincides with the translational speed of the table.

The developed forming system is shown in Figure 3. A CCD camera is installed in the system to capture the deformed shape of a rheological object. The captured image is sent to a PC and the motion of mechanism is determined based on the captured image.

3 Analysis of forming processes of rheological objects

In this section, we will investigate the forming process of rheological objects. Let us introduce an outline function to describe the deformed shape and develop a method to compute the outline function. Figure 4-(a) shows an example of grayscale images captured by the CCD camera. Note that the table surface is black and that the location of the table in a captured image is constant. Thus, we can easily extract the deformed shape of a rheological object, as shown in Figure 4-(b).

Let x_{max} be the width of the obtained image and y_{max} be its height. Let $p(i, j)$ be the grayscale at a lattice point (i, j) . Then, the gravity center of the deformed shape (X_g, Y_g) is given by

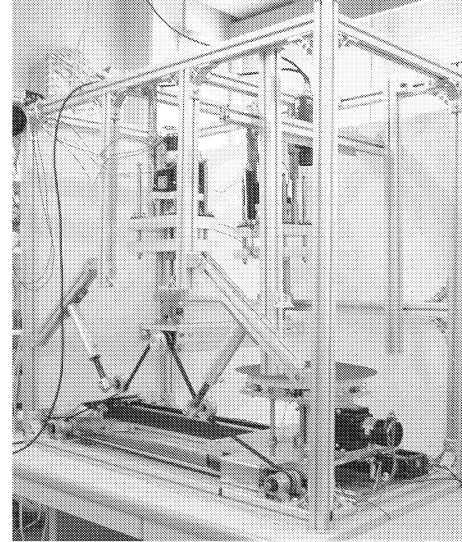


Figure 3: Prototype of forming system

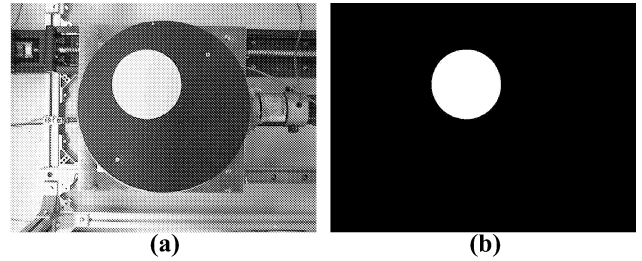


Figure 4: Images of rheological object :(a) Original image, (b) Extracted object image

$$\begin{bmatrix} X_g \\ Y_g \end{bmatrix} = \frac{1}{W} \sum_{i=0}^{x_{max}} \sum_{j=0}^{y_{max}} p(i, j) \begin{bmatrix} i \\ j \end{bmatrix}$$

where

$$W = \sum_{i=0}^{x_{max}} \sum_{j=0}^{y_{max}} p(i, j).$$

Let $f(\theta)$ be the distance from the gravity center to the contour of the deformed shape at angle θ from x -axis, as illustrated in Fig. 5. The deformed shape of a rheological object is then described by a function $f(\theta) (0^\circ \leq \theta \leq 360^\circ)$, which is referred to as an *outline function* of the deformed shape. Figure 6 shows an example of the outline function of a deformed shape. Figure 6-(a) is the deformed shape image and Figure 6-(b) is the outline function of that.

Let us investigate the forming processes of rheological objects. In the forming process, a cylindrical roller extend a rheological object, as illustrated in figure 7. Note that the location of the gravity center changes during a forming process, as illustrated in Figure 7. Thus, the distance between a point on the contour

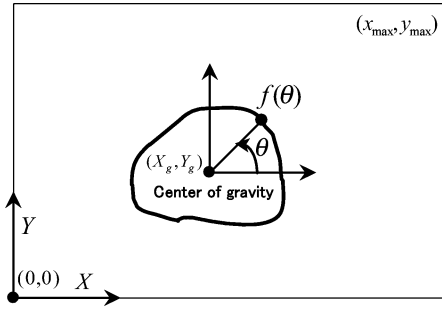


Figure 5: Outline function of deformed shape

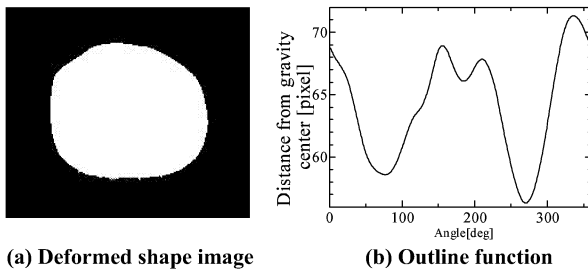


Figure 6: Example of outline function

and the gravity center may change during a forming process even if the point does not move. Thus, when a roller extends an object in one direction, the value of an outline function will increase at the roller angle as well as the value at the opposite roller direction after the forming.

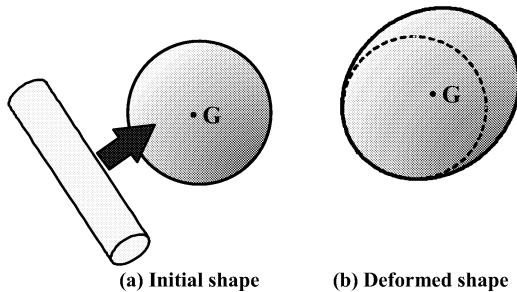


Figure 7: Extentional forming of rheological objects

Figure 8 shows a forming process of a circular rheological object of radius 47 mm. Figure 8-(a) is an initial shape and Figure 8-(b) is a deformed shape. The roller direction is given by 90° . Outline functions corresponding to the initial shape and the deformed shape are plotted in Figure 8-(c). As shown in the figure, the distance increases at angle 90° as well as at angle 270° . Consequently, we find that the value of an outline function increases at the roller direction and at the opposite direction.

Next, we will investigate the forming process of sim-

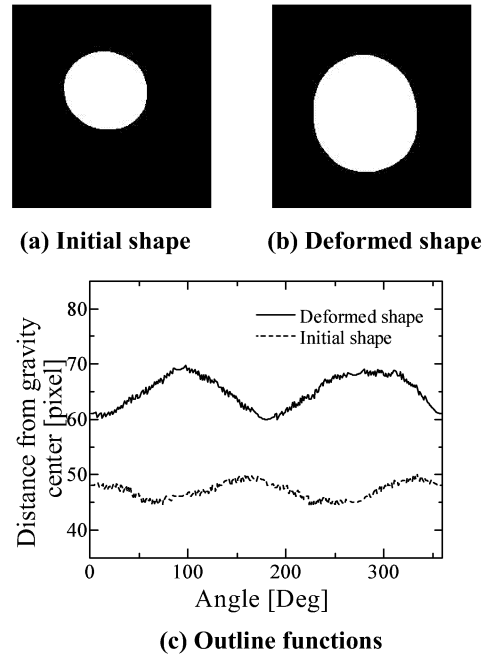


Figure 8: Forming of circular object of radius 47 mm

ilar initial shapes. Figure 9 shows a forming process of a circular rheological object of radius 57mm. Figure 9-(a) is an initial shape and Figure 9-(b) is a deformed shape. The roller direction is given by 90° . Outline functions corresponding to the initial shape and the deformed shape are plotted in Figure 9-(c). Initial shape given Figure 9-(a) is 1.2 times as large as the shape in Figure 8-(a). Let us normalize outline functions plotted in Figure 8-(c) by multiplying 1.2 so that they can be compared with the functions plotted in Figure 9-(c).

Normalized outline functions are plotted in Figure 10. Solid lines describe the forming process of a circular object with radius 47 mm. Broken lines describe the forming process of a circular object with radius 57 mm. From the figure, we find that the deformed shapes are similar each other when the initial shapes are similar. Consequently, it turns out that the forming processes preserve the similarity of deformed shapes.

4 Deformation Transition Graphs

4.1 Description of Forming Processes

In this section, we will introduce a deformation transition graph to describe the forming process of rheological objects. Since the proposed forming machine has multi degrees-of-freedom, it is required to determine a series of actions of the forming machine to perform a given forming operation of rheological objects successfully. Deformation transition graphs are useful to determine a series of actions for the forming machine.

One action of the forming machine yields a tran-

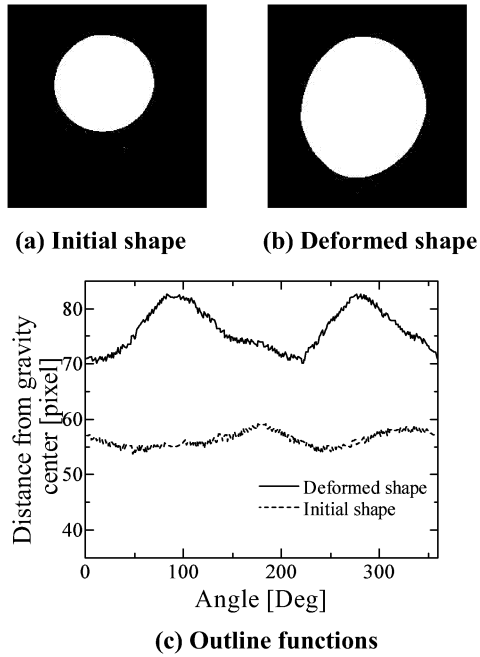


Figure 9: Forming of circular object of radius 57 mm

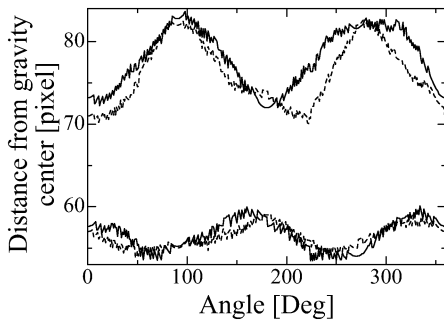


Figure 10: Normalized outline functions corresponding to forming processes of similar objects

sition from one shape to another of a rheological object. This implies that an action of the forming machine corresponds to a transition between one shape to another. Let us investigate whether an appropriate action of the forming machine yields a transition from one shape to another or not. For example, forming of a rheological object from the shape S_1 shown in Figure 11-(a) into the shape S_4 shown in Figure 11-(d) can be performed by moving the roller horizontally. On the other side, forming from the shape S_1 into the shape S_5 shown in Figure 11-(e) cannot be performed by any action of the forming machine. Namely, some transitions among shapes can be performed by actions of a forming machine and the other transitions are not possible.

Let us classify all actions of a forming machine into

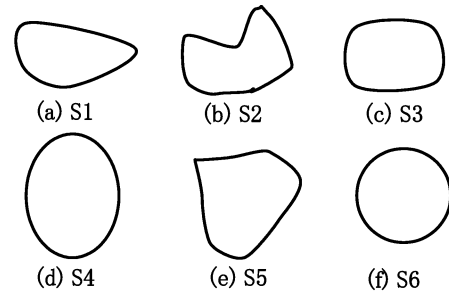


Figure 11: Examples of different shapes of rheological object

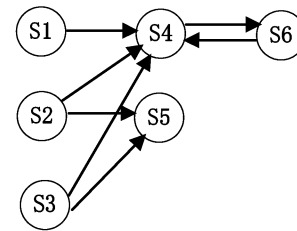


Figure 12: Deformation transition graph

a finite number of categories. Each category is represented by one action involved in the category. Then, one shape of a rheological object can be formed into a finite number of shapes by representative actions. Let us describe the relationship between the representative forming actions and deformation of a rheological object using a graph, as illustrated in Figure 12. A node of the graph describes a shape of a rheological object and an arc between two nodes denotes a representative forming action, where the object deforms from one shape corresponding to the starting node into the other corresponding to the end node. This graph is referred to as a *deformation transition graph*. Determination of a series of actions from the initial shape to the goal shape results in path finding from one node of the graph corresponding to the initial shape into another node corresponding to the goal shape. Consequently, deformation transition graphs are useful to plan the forming operations of rheological objects.

4.2 Feature extraction of outline function

In this section, we will classify deformed shapes of a rheological objects to define the nodes of a deformation transition graph. In the extensional forming of a rheological object, a roller approaches to the object toward its concave regions or toward its convex regions, as illustrated in Figure 13. This implies that concave regions and convex regions of a deformed shape are essential in the extensional forming. Thus, we will classify deformed shapes by concavity and convexity of the shapes.

Let us explain the classification using a simple outline function $f(\theta)$ plotted in Figure 14-(a). Note that a concave region of a deformed shape corresponds to a local minimum of an outline function and its convex

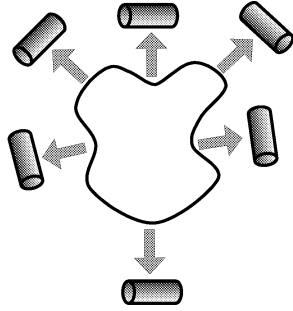


Figure 13: Possible directions of roller in extensional forming

region corresponds to a local maximum of the function. Here, we will focus on two local minima, say, the smallest one and the second smallest one as well as on two local maxima, say, the largest one and the second largest one. Without losing the generality, we assume that an outline function takes its maximum value at $\theta = 0$. Assume that the function takes its minimum value at $\theta = \alpha$. Let us examine the value of the function at the two local minima and at the two local maxima. In order to describe the function qualitatively, let us divide the range of the outline function as follows:

$$\begin{aligned} \text{region 1} &= [f(0) - d, f(0) + d], \\ \text{region 2} &= [f(\alpha) + d, f(0) - d], \\ \text{region 3} &= [f(\alpha) - d, f(\alpha) + d] \end{aligned}$$

where $d = (f(0) - f(\alpha))/4$. We will examine which region the value of the function is involved in at the two local minima and at the two local maxima. For example, the value of an outline function given in Figure 14-(a) involved in region 2 at the second largest local maximum and at the second smallest local minimum. The numbers of regions corresponding to the four local extreme points are listed in order to describe the function qualitatively. The function plotted in Figure 14-(a) is then symbolized as [1322]. These symbols correspond to individual nodes of a deformation transition graph. Note that the maximum of an outline function is always involved in region 1. Consequently, we have $3^3 = 27$ nodes in a deformation transition graph. Figure 14-(b) shows an outline function, which is symbolized as [1223].

4.3 Determination of forming actions

In this section, we will determine forming actions, which represent arcs in a deformation transition graph. Here, we will focus on the angle of the table of a forming machine, ψ , and the height of the roller, D . As mentioned in the previous section, the direction of a roller corresponds to four local extremes of an outline function. Thus, we will determine angle ψ so that the direction of a roller satisfy this condition.

Next, let us investigate how to determine the height of a roller, D . As mentioned in Section 3, a forming action can preserve the similarity of deformed shapes.

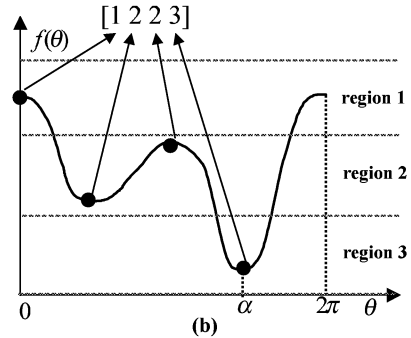
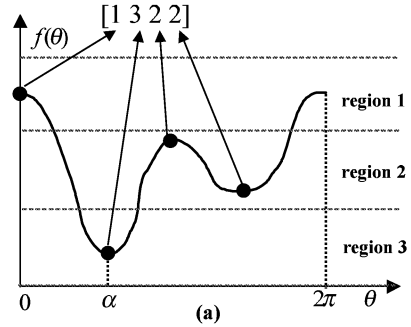


Figure 14: Symbolic representation of deformed shapes

Forming actions that preserve this similarity are useful in the determination of forming actions since we do not have to deal with the absolute values of action variables, say, ψ and D . Thus, we will focus on forming actions that preserve the similarity of deformed shapes.

Let $D_{present}$ be the present height of a roller and D_{next} be the height in the following action. Note that D_{next} must be determined so that the similarity is preserved. Thus, we will investigate an appropriate value of D_{next} corresponding to $D_{present}$ in advance experimentally. Namely, we will obtain function $D_{next} = D_{next}(D_{present})$ through forming experiments. Once the function is obtained, we can determine the height D_{next} uniquely corresponding to the present height $D_{present}$.

5 Forming Control Using Deformation Transition Graphs

In this section, we will propose a control method for forming rheological object using a deformation transition graph.

Here, we will investigate a forming of pizza dough into a circular shape. Goal node of a deformation transition graph in this forming is denoted by [1111], as illustrated in Figure 15. One action should be determined at any node except the goal node so that the deformed shape can be guided to the goal shape. In this forming, an action where the roller approaches toward the smallest local minimum is selected at any node but the goal node.

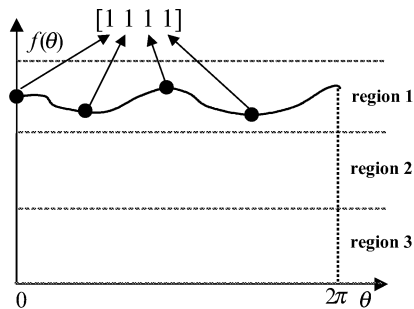


Figure 15: Outline function at goal node

Figure 16 shows an example of the forming. Figure 16-(a) through (f) describe the deformed shapes of a rheological object at individual iterations during the forming. The object consists of wheat flour and water in weight ratio 1:3. Figure 17 provides the corresponding outline functions. From these figures, we find that the rheological object can be formed into a circular shape successfully.

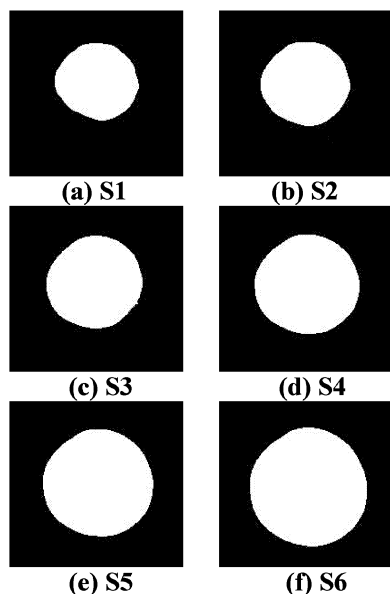


Figure 16: Deformed shapes of dough at individual iterations

6 Concluding Remarks

In this article, we have proposed a control method in the vision-based forming of rheological objects. First, we have developed forming machine of rheological objects with multi degrees-of-freedom. Secondly, we have analyzed the forming processes of rheological objects. Thirdly, we have introduced a deformation transition graph so that the forming processes can be described in a systematic manner. Finally, we have

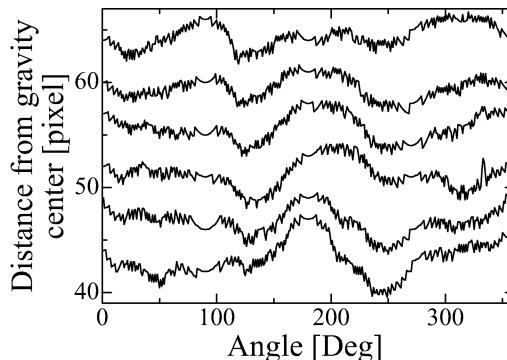


Figure 17: Outline functions at individual iterations

proposed a forming control method of a rheological object based on the deformation transition graph.

Future issues include (1) experimental evaluation of the robustness of the proposed method against the variation of object properties, (2) forming of rheological objects into a shape except circle, and (3) optimization of series of forming actions.

References

- [1] Terzopoulos, D., and Fleisher, K., *Modeling Inelastic Deformation: Viscoelasticity, Plasticity, Fracture*, Computer Graphics, Vol.22, No.4, pp.269–278, Albuquerque, May, 1988
- [2] Joukhader, A., Deguet, A., and Laugie, C., *A Collision Model for Rigid and Deformable Bodies*, Proc. IEEE Int. Conf. on Robotics and Automation, pp.982–988, Albuquerque, May, 1998
- [3] Chai, Y., and Luecke, G. R., *Virtual Clay Modeling Using the ISU Exoskeleton*, Proc. IEEE Virtual Reality Annual Int. Symp., pp.76–80, 1998
- [4] Barnes, H. A., Hutton, J. F., and Walters, K., *An Introduction to Rheology*, Elsevier Science Publishers, 1989
- [5] Taylor, P. M., eds., *Sensory Robotics for the Handling of Limp Materials*, Springer-Verlag, 1990
- [6] Henrich, D., and Wörn, H. eds., *Robot Manipulation of Deformable Objects*, Springer-Verlag, Advanced Manufacturing Series, 2000
- [7] Zheng, Y. F., Pei, R., and Chen, C., *Strategies for Automatic Assembly of Deformable Objects*, Proc. IEEE Int. Conf. on Robotics and Automation, pp.2598–2603, 1991
- [8] Hirai, S., Wada, T., *Indirect Simultaneous Positioning of Deformable Objects with Multi Pinching Fingers Based on Uncertain Model*, Robotica, Millennium Issue on Grasping and Manipulation, Vol.18, pp.3-11, 2000
- [9] Tokumoto, S., Fujita, Y., and Hirai, S., *Deformation Modeling of Viscoelastic Objects for Their Shape Control*, Proc. IEEE Int. Conf. on Robotics and Automation, Vol.1, pp.767–772, Detroit, May, 1999